Published in final edited form as:
Exp Neurol. 2011 October ; 231(2): 236–246. doi:10.1016/j.expneurol.2011.06.015.

Matrix metalloproteinase-9 controls proliferation of NG2+ progenitor cells immediately after spinal cord injury

Huaqing Liu[1,2] and **Veronica Shubayev**[1,2]

[1]Department of Anesthesiology at the University of California, San Diego

[2]VA San Diego Healthcare System, La Jolla, CA

Abstract

We have demonstrated that overcoming matrix metalloproteinase (MMP)-mediated suppression of glial proliferation stimulates axonal regeneration in the peripheral nervous system. The regenerative capacity of the adult CNS in response to injury and demyelination depends on the ability of multipotent glial NG2+ progenitor cells to proliferate and mature, mainly into oligodendrocytes. Herein, we have established the important role of MMPs, specifically MMP-9, in regulation of NG2+ cell proliferation in injured spinal cord. Targeting transiently induced MMP-9 using acute MMP-9/2 inhibitor (SB-3CT) therapy for two days after T9-10 spinal cord dorsal hemisection produced a significant increase in mitosis (assessed by bromodeoxyuridine incorporation) of NG2+ cells but not GFAP+ astrocytes and Iba-1+ microglia and/or macrophages. Acute MMP-9/2 blockade reduced the shedding of the NG2 proteoglycan and of the NR1 subunit of the N-methyl D-aspartate (NMDA) receptor, whose decline is believed to accompany NG2+ cell maturation into OLs. Increase in post-mitotic oligodendrocytes during remyelination and improved myelin neuropathology in the hemisected spinal cord were accompanied by locomotion and somatosensory recovery after acute MMP-9/2 inhibition. Collectively, these data establish a novel role for MMPs in regulation of NG2+ cell proliferation in the damaged CNS, and a long-term benefit of acute MMP-9 block after SCI.

INTRODUCTION

Neuron-glial antigen 2 (NG2)-expressing cells are multipotent glial progenitor cells of the resting CNS that give rise to oligodendrocytes (OLs) and other glia (Horner et al., 2000; Dawson et al., 2003; Zhu et al., 2008), and by receiving synaptic input from neurons are believed to integrate in the neuronal network (Nishiyama et al., 2009). In response to injury and demyelination of spinal cord, NG2+ cell division serves to replenish the pool of dying OLs and to support remyelination of the damaged CNS (McTigue et al., 2001). Despite the multipotent nature, NG2+ cells primarily commit to the OL lineage in healthy and degenerating spinal cord (Kang et al., 2010).

A chondroitin sulfate proteoglycan 4, NG2 is inhibitory to axonal growth (Giger et al., 2010). Yet, regenerating spinal cord axons associate preferentially with NG2-rich substrates (Jones et al., 2002) and NG2+ cells provide a favorable substrate for growing axons (Yang

Correspondence to: Dr. Veronica Shubayev, Department of Anesthesiology, University of California, San Diego, School of Medicine, 9500 Gilman Dr., Mailbox 0629, La Jolla, CA 92093-0629. Phone: (858) 534-3886, Fax: (858) 534-1445, vshubayev@ucsd.edu.

et al., 2006a). It is believed that not the membrane-anchored, but a shed isoform of NG2 proteoglycan evokes growth-inhibitory properties (Nishiyama et al., 2009; Jones et al., 2003). During the macrophage-induced axonal dieback, NG2+ cells stabilize axonal growth and form permissive bridges across proteoglycans (Busch et al., 2010). Both NG2 shedding in the spinal cord (Larsen et al., 2003) and axonal dieback (Busch et al., 2010) are controlled by matrix metalloproteinase-9 (MMP-9, or gelatinase B).

MMPs belong to a family of zinc-dependent extracellular endopeptidases, comprising collagenases, gelatinases, stromelysins and membrane-type MMPs (Nagase et al., 2006). By proteolysis of extracellular and membrane-bound adhesion and structural molecules, proteoglycans, cytokine and trophic factor ligands and receptors (Page-McCaw et al., 2007), or by direct receptor binding (Piccard et al., 2007), MMPs control a plethora of signal transduction pathways to phenotypic transformation, migration and survival. At least ten MMP family members are induced over the course of SCI (Wells et al., 2003), but their function remains poorly characterized. It is, however, clear that acute but not extended broad-spectrum MMP inhibitor (MMPi) therapy is effective in promoting functional recovery after SCI (Noble et al., 2002). The extended MMPi therapy fails the repair due to beneficial roles of certain MMPs, such as MMP-2, in wound healing at later stages of SCI (Hsu et al., 2006; Zhang et al., 2010).

The success of acute MMPi therapy has been attributed to blocking MMP-9-mediated vascular instability and immune cell recruitment (Noble et al., 2002; Yu et al., 2008), neuronal apoptosis (Yu et al., 2008) and glial scar formation (Hsu et al., 2008) after SCI. In dorsal root ganglia (DRG) neurons cultured on aggrecan, MMP-9 inhibition stimulates axonal growth by preventing macrophage attack of growth cones (Busch et al., 2009). We have reported that MMP inhibition facilitates axonal growth of DRG neurons in sciatic nerve *in vivo*, by stimulating proliferation of supporting Schwann cells (Liu et al., 2010). Unlike other MMP family members, MMP-9 is not expressed in resting adult spinal cord but induced transiently between 24 and 72 h after SCI (Noble et al., 2002; Yu et al., 2008; Duchossoy et al., 2001). Whether MMP-9 contributes to the later stages of SCI (Zhang et al., 2010) or controls myelin catabolism and/or formation in the damaged CNS (Rosenberg, 2009) remains controversial.

Herein, we demonstrate that selective, acute MMP-9/2 (SB-3CT) inhibition for two days after spinal cord dorsal hemisection acts as a mitogen for NG2+ cells but not GFAP+ astrocytes or Iba-1+ macrophages and/or microglia. In the damaged spinal cord, the MMPs control the shedding of NG2 proteoglycan, and of the NR1 subunit of the N-methyl D-aspartate receptor (NMDAr), whose decline is believed to accompany NG2+ cell maturation into OLs (De Biase et al., 2010). Finally, acute MMP-9/2 block permits successful post-mitotic maturation of OLs, improves neuropathology of myelin, and facilitates functional (locomotion and somatosensory, bladder) recovery associated with the lesion. Results from this study identify MMP-9 as a novel modulator of NG2+ cell proliferation in CNS, and support a paradigm that MMP-9 action early after SCI has major long-term implications to the course of spinal cord repair.

MATERIALS AND METHODS

Animals and surgery

Thoracic (T) 9-10 spinal cord dorsal hemisection (SCDH) was performed in adult female Sprague-Dawley rats (200-225 g, Harlan Labs, Indianapolis, IN). Animals were housed at 22°C under a 12 h light/dark cycle with *ad libitum* access to food and water. Deep anesthesia was achieved using a rodent anesthesia cocktail containing Nembutal (50 mg/ml; Abbott Labs, North Chicago, IL) and diazepam (5 mg/ml, Steris Labs, Phoenix, AZ) in 0.9% saline

(Steris Labs). Following laminectomy at T9-10 level, the dura mater was pierced, the spinal cord was exposed, and a pledget of Gelfoam soaked in saline was placed on the exposed cord for 1 min. A dorsal hemisection was performed with a stereotaxically positioned blade to a depth of 1.0 mm (as illustrated in Fig. 1A), fully severing the dorsal and dorsolateral corticospinal tracts (Weidner et al., 2001). The overlying muscle was sutured with 4.0 vicryl, and the skin was closed with surgical staples. Sham-operated animals underwent laminectomy without the lesion. Animals were allowed to recover from anesthesia on a heating pad. Ampicillin (30 mg/kg, APP Pharmaceuticals, Schaumburg, IL) was administered by intraperitoneal (i.p.) injection for seven days after injury. Bladders were expressed twice daily until the animals resumed eating and drinking normally and urinary incontinence ceased. All procedures conform to NIH Guidelines for the Care and Use of Laboratory Animals and protocols approved by the Institutional Animal Care and Use Committee and the VA San Diego Healthcare System.

MMP inhibitor therapy

SB-3CT (EMD Biosciences, San Diego, CA) is the selective, mechanism-based and high-affinity inhibitor of gelatinases with Ki values of 0.0139 μM for MMP-2 and 0.6 μM for MMP-9, and Ki values of 15-205 μM for MMP-1, MMP-3, and MMP-7 (Brown et al., 2000). SB-3CT (10 mg/kg body weight) as a suspension in 10% DMSO has been shown effective in protecting neurons from apoptosis during focal cerebral ischemia (Gu et al., 2005) and SCI (Yu et al., 2008). SB-3CT was injected i.p. immediately after SCDH and once daily for two days thereafter. 10% DMSO in normal saline was used as a vehicle control.

Real-time qRT-PCR

Spinal cords were collected at days 1, 3 and 7, at the epicenter of T9-10 SCDH and stored in RNA-later (Ambion, Austin, TX) at -20°C. Primers and *Taqman* probes for rat MMP-9 (Biosearch Technologies, Novato, CA), MMP-2 (Ambion) and glyceraldehyde 3-phosphate dehydrogenase (GAPDH, Biosearch Technologies) were optimized as described (Shubayev et al., 2006). Total RNA was extracted with Trizol (Invitrogen, Carlsbad, CA), purified on RNeasy mini columns (Qiagen, Valencia, CA) and treated with RNase-free DNAse I (Qiagen). The RNA purity was verified by OD260/280 absorption ratio of ~ 2.0. cDNA was synthesized using a SuperScript first-strand RT-PCR kit (Invitrogen). Gene expression was measured by real-time quantitative RT-PCR (MX4000, Stratagene, La Jolla, CA) using 50 ng of cDNA and 2x Taqman Universal PCR Master Mix (Ambion) with a one-step program: 95°C for 10 min, 95°C for 30 sec, and 60°C for 1 min for 50 cycles. Duplicate samples without cDNA (no-template control) showed no contaminating DNA. Relative mRNA levels were quantified using the comparative delta delta Ct method (Livak and Schmittgen, 2001) and GAPDH as a reference gene. A fold change between injured and naïve cords was determined by the MX4000 software as described (Pfaffl, 2001).

Gelatin zymography

Spinal cords were collected at day 1, at the epicenter of T9-10 SCDH and SB-3CT therapy and homogenized in non-reducing buffer (63 mM Tris–HCl, 10% glycerol and 2% SDS, pH 6.8). The lysates containing 25 mg of cord tissue were subjected to 10% SDS-PAGE containing 1 mg/ml of gelatin (Novex, San Diego, CA) at 160 V for 90 min. The proteins were renatured in 2.5% Triton X-100 twice for 20 min, and the gels were incubated at 37°C for 20 h in Zymogram Developing buffer (Novex), containing 50 mM Tris Base, 40 mM 6 N HCl, 200 mM NaCl, 5 mM $CaCl_2$ and 0.2% Brij 35. The gels were stained with colloidal blue (Novex), indicating gelatinolytic activity as a clear zone on a blue background of undegraded gelatin.

Immunoblotting

Spinal cords were collected at days 3, at the epicenter of T9-10 SCDH, snap-frozen in liquid N_2, and stored at -80°C. Proteins were extracted in 50 mM Tris-HCl, pH 7.4, containing 1% Triton-x 100, 150 mM NaCl, 10% glycerol, 0.1% SDS, 5 mM EDTA, 1 mM PMSF, 1 μg/mL aprotinin and leupeptin. Lysates containing 20 μg of total protein, as detected by BCA Protein Assay (Pierce, Rockford, IL), were separated on 10% Tris-glycine SDS-PAGE (Bio-Rad, Hercules, CA) at 50 to 80 mA, and transferred to nitrocellulose using iBlot dry blotting system (Invitrogen) at 20 V for 7 min. The membranes were blocked with 5% non-fat milk (Bio-Rad), followed by incubation with polyclonal rabbit antibody to a carboxyl-terminus of rat NR1 (Millipore (06-314); 1:2000, Temecula, CA), polyclonal rabbit anti-NG2 (Millipore (AB5320), 1:1000) and polyclonal rabbit anti-human IGFBP-6 (Santa Cruz (sc-13094), 1:400) antibodies in 5% bovine serum albumin (Sigma, St. Louis, MO) overnight at 4°C, washed in TBS containing 0.1% Tween and incubated for 1 h at room temperature (RT) with HRP-conjugated anti-rabbit secondary antibody (Cell Signaling; 1:5000, Danvers, MA). The blots were developed using enhanced chemiluminescence (Amersham, Arlington Heights, IL). The membranes were reprobed with mouse anti-β-actin antibody (Sigma; 1:10000) to control protein loading. Optical density (OD) of the bands of interest was measured in N of 4 per group using Image J 1.38u (NIH, Bethesda, MD).

In vivo BrdU labeling and detection

5-bromo-2-deoxyuridine (BrdU, Calbiochem, San Diego, CA, 50 mg/kg/day) or its vehicle (1 mM Tris, 0.8% NaCl, 0.25 mM EDTA, pH 7.4) was administered i.p. immediately after SCDH or sham surgery and daily for 2 days thereafter. At 3 and 21 days after SCDH and injections, animals were anesthetized, perfused with 4% paraformaldehyde and sacrificed by exsanguination. Spinal cords were isolated, post-fixed overnight, rinsed, cryoprotected in graded sucrose, embedded into OCT compound in dry ice. Transverse, free-floating 25-μm-thick sections were cut and stored in frozen buffer containing 25% glycerin and 30% ethylene glycol in 0.1 M phosphate buffer. The sections were rinsed in PBS, hydrolyzed in 2N HCl in PBS for 30 min, followed with or without digestion with 0.01% Trypsin for 30 min at 37°C and washed with PBS. Non-specific binding was blocked in solution containing PBS, 5% normal goat serum and 0.25% Triton X-100, followed by mouse anti-BrdU antibody (Sigma (B2531), 1:200) overnight at 4°C, PBS rinse and goat anti-mouse Alexa 488 (green) antibody (Invitrogen) treatment for 1 h at RT. Sections were mounted and coverslipped using slowfade (Invitrogen).

BrdU dual-labeling with phenotypic markers—The spinal cord sections were first stained with rat anti-BrdU (Abcam (ab6326), 1:100, Cambridge, MA) or mouse anti-BrdU as described above, followed by the respective secondary goat anti-rat or anti-mouse Alexa 488 (green), and an overnight incubation at 4°C with one of the following second primary antibodies: polyclonal rabbit anti-rat NG2 (Millipore (AB5320), 1:200), polycolonal rabbit anti-glial fibrillary acidic protein (GFAP, Dako (Z0334), 1:1000, Carpinteria, CA), rabbit anti-Iba-1 (Wako (019-19741), 1:200, Richmond, VA), rabbit anti-S100 (Dako (Z0311), 1:500), monoclonal mouse anti-rat Rip (Millipore (MAB1580), 1:1000), monoclonal mouse anti-APC end-binding protein 1 (APCbp, BD Biosciences (610534) 1:500). Sections were rinsed in PBS and incubated with goat anti-rabbit Alexa 594 (red, Invitrogen) antibody for 1 h at RT. The primary antibody was replaced with the respective normal IgG to control signal specificity.

Quantitative morphometry—Imaging was performed using a Leica DMR bright-light and fluorescent microscope and Openlab 4.04 imaging software (Improvision Inc., Waltham, MA). BrdU+ cells (single- or dual-labeled with markers) were analyzed in spinal cord segments 1-3 mm caudal from the epicenter, the main region of BrdU incorporation

(Zai and Wrathall, 2005). Quantification was performed in N of 4-7 animals per group, every sixth 25-μm-thick transverse, dorsal column and dorsal horn section, 3 areas per section, photographed at 20x or 40x objective magnification. Cells were considered BrdU+ only when clearly present within the nucleus with a homogenous or clear punctate labeling pattern. Data was expressed as the number of immunostained cells per spinal cord area.

Myelin neuropathology

Myelin content was evaluated by light microscopy in fixed-frozen by *Luxol Fast Blue* staining or araldite-embedded, *Methylene Blue* stained spinal cord. For *Luxol Fast Blue* staining, OCT-embedded (25-μm-thick) transverse sections were incubated in 0.1% Solvent blue 38 (Sigma) overnight at 56°C, destained with 0.05% lithium carbonate, and counterstained with hematoxylin (Fisher Scientific, Pittsburgh, PA) and eosin (Sigma). For *Methylene Blue* staining, animals were perfused with 2.5% glutaraldehyde (Fisher) in 0.1 M phosphate buffer, pH 7.4, under rodent cocktail anesthesia cocktail, specified above. The spinal cords were isolated, postfixed for 48 h, osmicated, dehydrated, and embedded in araldite resin. Transverse (1-μm-thick) sections were cut with a diamond knife on an automated Leica RM2065 microtome and stained with Methylene Blue Azure II (Sigma) (Shubayev et al., 2006).

BBB locomotion testing

Locomotor activity was tested daily, starting one day after T9-10 SCDH for 22 days using the Basso-Beattie-Bresnehan (BBB) scale (Basso et al., 1995). The BBB scale characterizes specific features of functional behavior such as limb movement, paw placement/position, stepping, coordination, toe clearance and tail position. A score of 0 was given when no spontaneous hindlimb movement was observed, whereas a score of 21 was assigned to normal locomotion. The locomotor activity of individual animals was evaluated in an open field, consisting of a molded-plastic circular enclosure with a smooth, nonslippery floor (90-cm diameter; 18-cm wall height), over 4 min intervals by two experienced examiners. Testing was performed in *N* of 8-11 per group by an experimenter unaware of the experimental groups.

Bladder assessment

Animals received manual bladder expression twice daily after T9-10 SCDH and/or MMPi therapy. The bladder functional recovery was evaluated using the reported scale (Siegenthaler et al., 2007). Briefly, animals that required bladder expression were given a score of zero. Animals that did not require bladder expression, as determined by a relaxed bladder with minimal urine release during manual bladder expression, were given a score of one in *N* of 6 per group by an experimenter unaware of the experimental groups. Scores were summed per group for each time point, and a percentage of recovered bladder function was determined by dividing the sum of the scores by the number of animals per each group.

Statistical analysis

Statistical analyses were performed using KaleidaGraph 4.03 (Synergy Software, Reading, PA) or SPSS 16.0 (SPSS Inc, Chicago, IL) software by a two-tailed, unpaired Student's t-test. Analyses of variance (ANOVA) followed by Tukey-Kramer post-hoc test were employed for comparing three and more groups, and p values of < 0.05 were considered significant.

RESULTS

Transient MMP-9 expression in hemisected spinal cord

The expression levels of MMP-9 and MMP-2 as the potential targets of SB-3CT therapy was quantified at 1, 3 and 7 days of the T9-10 SCDH, using real-time *Taqman* qRT-PCR (Fig. 1B). MMP-9 expression peaked within 1 day of SCDH demonstrating an 8.27 ± 1.34-fold increase compared to naïve cord and a 6.07 ± 0.99-fold increase compared to sham-operated animals. MMP-9 levels declined by 3 days, and were not significantly different from sham at 7 days after SCDH. MMP-2 expression was elevated at 3 and 7 days after SCDH by 3.03 ± 0.39-fold and 3.45 ± 0.45-fold, respectively, relative to naïve spinal cord.

SB-3CT inhibits MMP-9 activity in spinal cord

Gelatin zymography confirms that at the peak of its mRNA expression (day 1 of SCDH), MMP-9 is active, and the SB-3CT (10 mg/kg, i.p.) administered immediately after SCDH effectively inhibits MMP-9 activity (Fig. 1C).

Acute SB-3CT therapy was administered immediately, and then once daily for 2 days after T9-10 SCDH based on the transient MMP-9 increase, and the reported efficacy of acute broad-spectrum MMPi therapy to spinal cord recovery (Noble et al., 2002). At 3-21 days following the surgery and therapy, the spinal cords were analyzed for BrdU+ profiles (Figs. 2-4) and MMP substrates, including NG2, NR1 and IGFBP-6 (Fig. 5) and myelin histopathology (Fig. 6). Behavioral analyses of functional recovery (Fig. 7) accompanied the study.

MMP-9 selectively controls mitosis of NG2+ cells

The cells undergoing mitosis were identified at day 3 after T9-10 SCDH following daily BrdU injection and acute SB-3CT therapy until day 2 of SCDH (Fig. 2A). Morphometric quantification of BrdU+ profiles was performed in the dorsal horn and column (Fig. 2B), as relevant to the lesion, in the segment 1-3 mm caudal to epicenter, the major zone of BrdU incorporation (Zai and Wrathall, 2005). The number of BrdU+ cells significantly elevated after SCDH, demonstrating a 14-fold increase relative to sham operation (Fig. 2C-D). Interestingly, at 214.8 ± 1.4 cells/area, SB-3CT therapy increased the rate of BrdU incorporation nearly 2-fold above that of vehicle treatment (at 114.5 ± 17.9 cells/area).

Next, the phenotype of the dividing cells was determined by dual-labeling BrdU with NG2, for NG2+ progenitors, GFAP for astrocytes or Iba-1 for microglia/macrophages (Fig. 3), as the key dividing cell types in the injured cord (McTigue et al., 2001; Yang et al., 2006b). The number of dividing NG2+ cells significantly increased in the acutely SB-3CT-treated group (53 ± 4 cells/area) compared to vehicle treatment (39 ± 4 cells/area) ($p<0.01$). Of the total BrdU+ profiles, dividing NG2+ cells represented 64% in MMPi-treated and 42% in vehicle-treated cords ($p<0.05$). A vast population of BrdU+ cells were Iba-1-reactive in both the vehicle and SB-3CT treated groups, although their levels were not significantly different between the groups. Mitotic GFAP+ cells were sparse in both groups, and thus, were not the focus for quantification. Collectively, phenotypic characterization of BrdU+ profiles suggests that selective and acute MMP-9/2 block differentially stimulates proliferation of NG2+ cells, but not astrocytes, macrophages and/or microglia within the first three days of the spinal cord injury.

NG2, NR1 and IGFBP-6, as MMP-9 substrates in the spinal cord

To advance our understanding on the effects of the acute MMP-9/2 block on the substrates known to modulate phenotypic plasticity of the OL cell lineage, we performed

immunoblotting for NG2, NR1 and IGFBP-6 (Fig. 4) upon completion of acute SB-3CT therapy at 3 days after SCDH, as illustrated in Fig. 2A.

NG2 chondroitin sulfate proteoglycan, a 270-300 kDa membrane protein, is a reported MMP-9 substrate in demyelinating spinal cord (Larsen et al., 2003). Its levels increased at 3 days of SCDH relative to sham (Fig. 4), yet the change was not significantly different when calibrated to the total (□-actin) protein. Acute SB-3CT treatment produced NG2 accumulation in the spinal cords relative to vehicle treatment.

Decline in NMDAr accompanies maturation of NG2+ cell into OLs (De Biase et al., 2010). The NR1 subunit of NMDAr is a substrate for MMP proteolysis that forms a ~38 kDa digest product (Pauly et al., 2008; Szklarczyk et al., 2008). A full-length, 120 kDa NR1 and a ~58 kDa carboxyl-terminal domain was detected in naïve and sham-operated spinal cords (Fig. 4). A ~38 kDa NR1 was evident at 3 days after SCDH in the vehicle-treated spinal cords, and its levels were significantly reduced after SB-3CT therapy.

IGFBP-6 is an MMP-9 substrate in brain, which by controlling bioavailability of IGF-1, can regulate maturation of oligodendrocytes progenitors (Larsen et al., 2006). The changes in IGFBP-6 were not significantly different between any of the experimental groups (Fig. 4).

The fate of post-mitotic cells in SB-3CT-treated remyelinating cords

Since OLs are the preferred destination for post-mitotic NG2+ cells (Kang et al., 2010), the fate of BrdU+ cells was followed to remyelination at 3 weeks of SCI (Griffiths and McCulloch, 1983). BrdU was administered until 2 days of SCDH, as described above, and traced to 21 days of SCDH, as illustrated in Fig. 5A. Mature OLs were identified with Rip (Horner et al., 2000) and dual-labeled with BrdU, demonstrating increased content in SB-3CT-treated compared to vehicle-treated cords (Fig. 5B-C). Because Rip staining makes it difficult to discern individual cells, adenomatous polyposis coli (APC) end-binding protein 1 (APCbp) that binds to APC in cytosol (Nakamura et al., 2001) and co-localizes with myelin basic protein and myelin associated glycoprotein of spinal cord (not shown), was dual-labeled with BrdU, demonstrating significant increase in BrdU/APCbp content in SB-3CT-treated compared to vehicle-treated cords (Fig. 5B-C). A vast population of Iba-1+ cells co-localized with BrdU at 21 days of injury, but their levels remained not significantly different between the groups, representing 54.7 and 58.6% of the total BrdU+ population, respectively (Fig. 5B-C). Because NG2 cells differentiate into astrocytes (Lytle and Wrathall, 2007; Alonso, 2005) and Schwann cells (Zawadzka et al., 2010), and the latter express Rip (Toma et al., 2007) and may contribute to Rip+ profiles (above), BrdU was dual-labeled with S100 and GFAP. Both S100+ and GFAP+ cells were detectable in the spinal cord segment at 21 days after SCDH, but minimally co-distributed with BrdU (Fig. 5, B).

Acute MMP-9/2 block improves neuropathology of myelin

The effect of acute SB-3CT block on myelin content was assessed at 3-21 days after SCDH in the spinal cord segments 1-3 mm caudal to epicenter, where BrdU+ profiles had been characterized. In vehicle-treated SCDH cords, myelin integrity was weakened by 3 days, displaying pronounced demyelination in the caudal segment at 14 days SCDH (Fig. 6A). Remyelination was evident by 21 days, as noted by accumulation of myelin (Fig. 6A, blue) and clusters of densely packed areas of small-diameter axons, surrounded by the thin rim of myelin sheaths in araldite-embedded cords (Fig. 6B). The SB-3CT-treated SCDH cords maintained relatively high myelin levels at every time-point, as compared to vehicle (Fig. 6A). The delay in de- and remyelination of the vehicle-treated cord observed here is likely to

relate to the caudal location of the sections relative to the lesion. Accumulation of myelin was particularly evident at 21 days of SCDH in the SB-3CT-treated cords (Fig. 6A-B).

Acute MMP-9/2 inhibition improves locomotion and somatosensory recovery

The effect of acute SB-3CT therapy on locomotion behavior was assessed daily using the BBB scale. As compared to sham operation, the T9-10 SCDH lesion produced an immediate and robust decline in BBB scores of vehicle-treated animals (Fig. 7A). In contrast, significant improvement of locomotion scores manifested immediately after the initiation of the SB-3CT therapy, and its protective effect lasted for the duration of the study.

Somatosensory recovery was evaluated by bladder function recovery in animals that received acute MMP-9/2 inhibition or vehicle treatment (Fig. 7B). Both groups required bladder expression for 2 days after SCDH. By 7 days of SCDH, up to 80% of rats undergoing SB-3CT therapy displayed recovered bladder function. In contrast, the vehicle-treated animals maintained a 50% recovery rate until day 10 after SCDH. By day 11, bladder function recovery was evident in 100% of SB-3CT-treated animals, while the recovery rate fluctuated until day 20 of SCDH with vehicle treatment.

DISCUSSION

The present study has established the novel role for MMPs in modulation of NG2-expressing cell division in the damaged CNS. Specifically, acute MMP-9/2 inhibitor (SB-3CT) administered immediately and then daily for two days after T9-10 SCDH: (1) increases the number of dividing NG2 (not GFAP or Iba-1)-reactive cells and the levels of NG2 proteoglycan; (2) increases the number of post-mitotic Rip and APCbp-reactive, presumably, oligodendrocytes in remyelinating cord; (3) prevents the shedding of the NR1 subunit of NMDAr, that rapidly declines with NG2 cell maturation (De Biase et al., 2010); (4) improves neuropathology of myelin, and (5) functional (locomotion and somatosensory) recovery from the lesion.

MMP-9, the target for acute SB-3CT therapy in spinal cord

SB-3CT is a mechanism-based, selective inhibitor to MMP-9 and MMP-2 (Brown et al., 2000). The two gelatinases are differentially induced in various models of SCI, as summarized by Zhang and colleagues (Zhang et al., 2010). The time-frame for the transient induction of MMP-9 mRNA between 24 and 72 h of SCDH that we observe in our study corresponds to the transient increase in its gelatinolytic activity in hemisected spinal cord (Duchossoy et al., 2001), other models of experimental SCI (Zhang et al., 2010), and in patients with traumatic SCI (Buss et al., 2007), where neutrophils (de Castro et al., 2000), astrocytes and endothelial cells (Noble et al., 2002; Zhang et al., 2010; Buss et al., 2007) are primary MMP-9 producers. MMP-9 has been identified as “a signature of the acutely injured cord” (Zhang et al., 2010), as MMP-2 expression presents constituently (de Castro et al., 2000) and remains at baseline until day 3 of SCDH, that is, after withdrawal of the SB-3CT therapy.

The ability of SB-3CT to prevent oxidative stress-induced neuronal apoptosis and blood-brain degradation, observed with intrathecal administration 2 h prior to SCI, has been attributed to MMP-9 inhibition (Yu et al., 2008). SB-3CT prevents neuronal apoptosis by protecting laminin from MMP-9 proteolysis during focal cerebral ischemia (Gu et al., 2005). Mouse SCI models in MMP-9 knockout background have established the essential role of MMP-9 in diminishing vascular integrity (Noble et al., 2002) and facilitating glial scar formation (Hsu et al., 2008). Given the high affinity of SB-3CT to MMP-2 (Brown et al., 2000), its contribution to the present findings may not be fully excluded.

MMP-9 as suppressor of NG2+ cell mitosis: Implications for the OL lineage

Acute MMP-9 inhibition increases the number of NG2 cells (via mitosis). Most recently, an endogenous MMP-9 inhibitor, TIMP-1, has proven essential to maintaining high numbers of NG2 cells in neurosphere cultures (Moore et al., 2011). In addition, TIMP-1 promotes NG2 cell differentiation into OLs (Moore et al., 2011), as acute MMP-9 block in our study increases the number of post-mitotic Rip and APC end-binding protein 1 expressing cells in remyelinating cords. Because NG2 cells divide effectively within the first days of SCI, when MMP-9 expression is high, we offer that MMP-9 works to limit, rather than prevent NG2 cells from entering the cell cycle, and that MMP-9-mediated effect on NG2 cell function depends on the context of the microenvironment in the spinal cord. Cultured NG2 cells employ MMP proteolysis for migration across inhibitory proteoglycans, although based on the Ki values and the dose of the MMPi required to achieve the anti-migratory effect, MMP-1 and MMP-13, but not MMP-9, have been implicated in the process (Busch et al., 2010). MMP-9 stimulates cultured OL to extend processes towards myelinating axons (Oh et al., 1999; Uhm et al., 1998). As OLs undergo vigorous apoptosis in degenerating cords (McTigue et al., 2001), the role of MMPs in OL survival need be assessed in future studies. Intriguingly, recombinant TIMP-1 but not broad-spectrum MMP inhibition evokes a dose-dependent increase in NG2 cell counts in neurosphere cultures from the TIMP-1 knockout mice (Moore et al., 2011), emphasizing not only the complexity of the TIMP-MMP system, but its potential effects, independent of the catalytic MMP function.

Catalytic and signaling roles of MMP-9 in spinal cord

MMP-9 is a multidomain protease which regulates cell signaling by catalytic and non-catalytic activation/inactivation of various signaling pathways (Piccard et al., 2007), of which little is known in cell systems related to SCI. Based on the ability of MMP-9 to process NG2 in OL *in vitro* (Larsen et al., 2003), the levels of NG2 proteoglycan (by immunoblotting) are increased in cords exposed to acute MMP-9/2 inhibition in the present study. Likewise, the spinal cords of MMP-9 knockout mice undergoing lysolecithin-induced demyelination accumulate immunoreactive NG2 (Larsen et al., 2003). Together, MMP-9-mediated control of NG2 proteolysis and NG2+ cell survival seem to be at play in the damaged spinal cord.

Decline in NMDAr accompanies NG2+ cell maturation into premyelinating OLs (De Biase et al., 2010). Formation of a 38 kDa MMP-digest of NR1 of the C-terminus ectodomain is thought to render the non-functional NMDAr due to removal of the glycine-binding pockets (Pauly et al., 2008). Thus, MMP-9-induced NR1 shedding may reflect a phenotypic switch of NG2+ cells to maturation, relate to NMDA-induced neuronal death (Manabe et al., 2005) or its many other functions in the injured spinal cord.

By proteolytic release of IGF-1 from IGFBP-6, MMP-9 is thought to promote myelination of the post-natal brain (Larsen et al., 2006). Although the tendency for the IGFBP-6 increase was noted in the adult cords acutely treated with the SB-3CT, the effect was not statistically significant. Mechanistic studies in the cultured NG2+ cells are required to elucidate the roles of MMP-9 in signaling and function, which it may regulate via plethora of anti-mitogenic factors. For example, in cultured Schwann cells the recombinant MMP-9 suppresses mitosis and activates ERK1/2 by regulation of the tyrosine kinase receptors, ErB and IGF-1 receptor (Chattopadhyay and Shubayev, 2009). Of interest is that Schwann cells can be a source of NG2 in spinal cord (Jones et al., 2003), and work together with OLs to regulate remyelination after SCI (Griffiths and McCulloch, 1983).

Remyelination after acute MMP-9/2 block vs MMP-9 gene deletion

After acute MMP-9/2 block, the hemisected spinal cords remyelinate successfully, whereas lysolecithin-stimulated cords of MMP-9 knockout mice fail to remyelinate (Larsen et al., 2003). The latter finding has been attributed to MMP-9-mediated NG2 accumulation, as a potential barrier for OL maturation. Because NG2 accumulates in spinal cords after both, MMP-9/2 block and MMP-9 gene deletion, alternative mechanisms should underlie their different remyelination patterns. In that regard it is important to point out that MMPi therapy targets catalytic MMP-9 function, whereas both catalytic and non-catalytic roles of MMP-9 (Piccard et al., 2007) may contribute to the knockout phenotype. Unlike acute MMP-2/9 block, the knockout MMP-9 background does not allow for selective targeting of the pathophysiologically relevant, transient upsurge of MMP-9 in spinal cord, and like extended MMPi therapy fails recovery after SCI (Noble et al., 2002). In addition, developmentally aberrant myelin of the MMP-9 knockout mice (Larsen et al., 2006) may complicate the studies of remyelinating adult cords. Myelin integrity is also expected to improve with MMPi, and possibly, MMP-9 knockout due to protection from MBP proteolysis (Gijbels et al., 1993; Proost et al., 1993) and demyelination (Rosenberg, 2009). We conclude that acute, selective MMP-9 block minimizes the adverse effects on remyelination observed with constitutive MMP-9 gene deletion.

MMPs in NG2+ cell functions outside myelination

NG2+ cells have the capacity to differentiate into astrocytes (Lytle and Wrathall, 2007; Alonso, 2005) and Schwann cells (Zawadzka et al., 2010), whose contribution to post-mitotic cell profiles are insignificant. This leads us to believe that the cells dividing within the first two days of SCI are not the major source of Schwann cell and astrocyte content of remyelinated cord, at least within the analyzed segment. Evidence there exists that NG2+ cells commit primarily to OL lineage in healthy and degenerating spinal cord (Kang et al., 2010).

MMP-9 facilitates scar formation by promoting astrocyte migration (Hsu et al., 2008). The NG2 proteoglycan, a major component of a glial scar, can be produced by macrophages in the damaged cord (Jones et al., 2002). Acute SB-3CT therapy produced no effect on the dividing (day 3) or post-mitotic levels (day 21) of Iba-1+ microglia and/or macrophages (albeit differential effect on the two cell types is conceivable). Likewise, Iba-1 reactivity in demyelinating cord of MMP-9 knockout mice was not significantly different from wildtype (Larsen et al., 2003). These data do not diminish the role of MMP-9 in macrophage infiltration or attack of sensory axonal growth cones during die-back (Busch et al., 2009; Busch et al., 2011). Characterization of MMP functions in spatial relation to a glial scar is important to consider for future studies.

NG2 cells support axonal growth (Jones et al., 2003; Busch et al., 2010). Quite likely, the SB-3CT effect to promote functional recovery relates to the increase in NG2+ cell number, as a growth-promoting force in injured cord. Likewise, MMPi therapy promotes peripheral nerve regeneration via pro-mitogenic action on supporting Schwann cells (Liu et al., 2010). The potential role of MMP-mediated maturation of APCbp reactive cells in APC-mediated microtubule cytoskeleton assembly in neurons (Rosenberg et al., 2008) deserves consideration. As shedding of the membrane-anchored NG2 creates inhibitory milieu to axonal growth (Nishiyama et al., 2009), MMPi-induced prevention of NG2 shedding may contribute to functional recovery observed in our study. As NG2+ cells receive synaptic input from neurons (Nishiyama et al., 2009), MMPs may influence (e.g., by NR1 shedding) the network integration.

MMP therapy for SCI

Acute, but not extended broad-spectrum (GM6001) MMPi therapy stimulates functional recovery of injured spinal cord SCI (Noble et al., 2002). Accordingly, we find acute MMP-9/2 blockade to facilitate locomotion and somatosensory (bladder) recovery. These findings are especially important, as beneficial MMP actions at later stages of SCI limit long-term use of MMPi compounds (Zhang et al., 2010), such as MMP-2 mediated promotion of wound healing (Hsu et al., 2006) or potential myelination of sensory DRG neurons (Lehmann et al., 2009). The potentially beneficial roles of MMP-9 in astrocyte migration (Hsu et al., 2008) and phenotypic shifts with the OL cell lineage, discussed above, need to be considered in scheduling MMP-9 blocking therapy, as well as the presently unknown functions of other family members, including MMP-3, 7, 10, 11,12, 13, 19 and 20, elevated in SCI (Wells et al., 2003). Compelling evidence exists for the efficacy of selective MMP-9 inhibition in spinal cord repair by vascular stabilization (Noble et al., 2002; Yu et al., 2008), suppression of neuronal apoptosis (Yu et al., 2008) and, potentially, limiting axonal dieback (Busch et al., 2009; Busch et al., 2011).

Conclusion—Herein, the first evidence that MMPs control NG2+ cell proliferation in the damaged CNS has emerged. Selective targeting of MMP-9 immediately after SCI increases the pool of NG2+ progenitors, allows for successful oligodendrocyte maturation and remyelination, and improves functional recovery of spinal cord.

Acknowledgments

The authors gratefully acknowledge Dr. Paul Lu at UCSD, Department of Neurosciences for providing guidance in spinal cord injury modeling and locomotion testing. This study was supported by NIH/NINDS R21NS060307 to VIS.

REFERENCES

Horner PJ, Power AE, Kempermann G, Kuhn HG, Palmer TD, Winkler J, Thal LJ, Gage FH. Proliferation and differentiation of progenitor cells throughout the intact adult rat spinal cord. J Neurosci. 2000; 20:2218–2228. [PubMed: 10704497]

Dawson MR, Polito A, Levine JM, Reynolds R. NG2-expressing glial progenitor cells: an abundant and widespread population of cycling cells in the adult rat CNS. Mol Cell Neurosci. 2003; 24:476–488. [PubMed: 14572468]

Zhu X, Bergles DE, Nishiyama A. NG2 cells generate both oligodendrocytes and gray matter astrocytes. Development. 2008; 135:145–157. [PubMed: 18045844]

Nishiyama A, Komitova M, Suzuki R, Zhu X. Polydendrocytes (NG2 cells): multifunctional cells with lineage plasticity. Nat Rev Neurosci. 2009; 10:9–22. [PubMed: 19096367]

McTigue DM, Wei P, Stokes BT. Proliferation of NG2-positive cells and altered oligodendrocyte numbers in the contused rat spinal cord. J Neurosci. 2001; 21:3392–3400. [PubMed: 11331369]

Kang SH, Fukaya M, Yang JK, Rothstein JD, Bergles DE. NG2+ CNS glial progenitors remain committed to the oligodendrocyte lineage in postnatal life and following neurodegeneration. Neuron. 2010; 68:668–681. [PubMed: 21092857]

Giger RJ, Hollis ER 2nd, Tuszynski MH. Guidance molecules in axon regeneration. Cold Spring Harb Perspect Biol. 2010; 2:a001867. [PubMed: 20519341]

Jones LL, Yamaguchi Y, Stallcup WB, Tuszynski MH. NG2 is a major chondroitin sulfate proteoglycan produced after spinal cord injury and is expressed by macrophages and oligodendrocyte progenitors. J Neurosci. 2002; 22:2792–2803. [PubMed: 11923444]

Yang Z, Suzuki R, Daniels SB, Brunquell CB, Sala CJ, Nishiyama A. NG2 glial cells provide a favorable substrate for growing axons. J Neurosci. 2006a; 26:3829–3839. [PubMed: 16597737]

Jones LL, Sajed D, Tuszynski MH. Axonal regeneration through regions of chondroitin sulfate proteoglycan deposition after spinal cord injury: a balance of permissiveness and inhibition. J Neurosci. 2003; 23:9276–9288. [PubMed: 14561854]

Busch SA, Horn KP, Cuascut FX, Hawthorne AL, Bai L, Miller RH, Silver J. Adult NG2+ cells are permissive to neurite outgrowth and stabilize sensory axons during macrophage-induced axonal dieback after spinal cord injury. J Neurosci. 2010; 30:255–265. [PubMed: 20053907]

Larsen PH, Wells JE, Stallcup WB, Opdenakker G, Yong VW. Matrix metalloproteinase-9 facilitates remyelination in part by processing the inhibitory NG2 proteoglycan. J Neurosci. 2003; 23:11127–11135. [PubMed: 14657171]

Nagase H, Visse R, Murphy G. Structure and function of matrix metalloproteinases and TIMPs. Cardiovasc Res. 2006; 69:562–573. [PubMed: 16405877]

Page-McCaw A, Ewald AJ, Werb Z. Matrix metalloproteinases and the regulation of tissue remodelling. Nat Rev Mol Cell Biol. 2007; 8:221–233. [PubMed: 17318226]

Piccard H, Van den Steen PE, Opdenakker G. Hemopexin domains as multifunctional liganding modules in matrix metalloproteinases and other proteins. J Leukoc Biol. 2007; 81:870–892. [PubMed: 17185359]

Wells JE, Rice TK, Nuttall RK, Edwards DR, Zekki H, Rivest S, Yong VW. An adverse role for matrix metalloproteinase 12 after spinal cord injury in mice. J Neurosci. 2003; 23:10107–10115. [PubMed: 14602826]

Noble LJ, Donovan F, Igarashi T, Goussev S, Werb Z. Matrix metalloproteinases limit functional recovery after spinal cord injury by modulation of early vascular events. J Neurosci. 2002; 22:7526–7535. [PubMed: 12196576]

Hsu JY, McKeon R, Goussev S, Werb Z, Lee JU, Trivedi A, Noble-Haeusslein LJ. Matrix metalloproteinase-2 facilitates wound healing events that promote functional recovery after spinal cord injury. J Neurosci. 2006; 26:9841–9850. [PubMed: 17005848]

Zhang H, Adwanikar H, Werb Z, Noble-Haeusslein LJ. Matrix metalloproteinases and neurotrauma: evolving roles in injury and reparative processes. Neuroscientist. 2010; 16:156–170. [PubMed: 20400713]

Yu F, Kamada H, Niizuma K, Endo H, Chan PH. Induction of mmp-9 expression and endothelial injury by oxidative stress after spinal cord injury. J Neurotrauma. 2008; 25:184–195. [PubMed: 18352832]

Hsu JY, Bourguignon LY, Adams CM, Peyrollier K, Zhang H, Fandel T, Cun CL, Werb Z, Noble-Haeusslein LJ. Matrix metalloproteinase-9 facilitates glial scar formation in the injured spinal cord. J Neurosci. 2008; 28:13467–13477. [PubMed: 19074020]

Busch SA, Horn KP, Silver DJ, Silver J. Overcoming macrophage-mediated axonal dieback following CNS injury. J Neurosci. 2009; 29:9967–9976. [PubMed: 19675231]

Liu H, Kim Y, Chattopadhyay S, Shubayev I, Dolkas J, Shubayev VI. MMP inhibition enhances the rate of nerve regeneration in vivo by promoting de-differentiation and mitosis of supporting Schwann cells. J Neuropathol Exp Neurol. 2010; 69:386–395. [PubMed: 20448483]

Duchossoy Y, Horvat JC, Stettler O. MMP-related gelatinase activity is strongly induced in scar tissue of injured adult spinal cord and forms pathways for ingrowing neurites. Mol Cell Neurosci. 2001; 17:945–956. [PubMed: 11414785]

Rosenberg GA. Matrix metalloproteinases and their multiple roles in neurodegenerative diseases. Lancet Neurol. 2009; 8:205–216. [PubMed: 19161911]

De Biase LM, Nishiyama A, Bergles DE. Excitability and synaptic communication within the oligodendrocyte lineage. J Neurosci. 2010; 30:3600–3611. [PubMed: 20219994]

Weidner N, Ner A, Salimi N, Tuszynski MH. Spontaneous corticospinal axonal plasticity and functional recovery after adult central nervous system injury. Proc Natl Acad Sci U S A. 2001; 98:3513–3518. [PubMed: 11248109]

Brown S, Bernardo MM, Li ZH, Kotra LP, Tanaka Y, Fridman R, Mobashery S. Potent and selective mechanism-based inhibition of gelatinases. J Am Chem Soc. 2000; 122:6799–6800.

Gu Z, Cui J, Brown S, Fridman R, Mobashery S, Strongin AY, Lipton SA. A highly specific inhibitor of matrix metalloproteinase-9 rescues laminin from proteolysis and neurons from apoptosis in transient focal cerebral ischemia. J Neurosci. 2005; 25:6401–6408. [PubMed: 16000631]

Shubayev VI, Angert M, Dolkas J, Campana WM, Palenscar K, Myers RR. TNFalpha-induced MMP-9 promotes macrophage recruitment into injured peripheral nerve. Mol Cell Neurosci. 2006; 31:407–415. [PubMed: 16297636]

Livak KJ, Schmittgen TD. Analysis of relative gene expression data using real-time quantitative PCR and the 2(-Delta Delta C(T)) Method. Methods. 2001; 25:402–408. [PubMed: 11846609]

Pfaffl MW. A new mathematical model for relative quantification in real-time RT-PCR. Nucleic Acids Res. 2001; 29:e45. [PubMed: 11328886]

Zai LJ, Wrathall JR. Cell proliferation and replacement following contusive spinal cord injury. Glia. 2005; 50:247–257. [PubMed: 15739189]

Basso DM, Beattie MS, Bresnahan JC. A sensitive and reliable locomotor rating scale for open field testing in rats. J Neurotrauma. 1995; 12:1–21. [PubMed: 7783230]

Siegenthaler MM, Tu MK, Keirstead HS. The extent of myelin pathology differs following contusion and transection spinal cord injury. J Neurotrauma. 2007; 24:1631–1646. [PubMed: 17970626]

Yang H, Lu P, McKay HM, Bernot T, Keirstead H, Steward O, Gage FH, Edgerton VR, Tuszynski MH. Endogenous neurogenesis replaces oligodendrocytes and astrocytes after primate spinal cord injury. J Neurosci. 2006b; 26:2157–2166. [PubMed: 16495442]

Pauly T, Ratliff M, Pietrowski E, Neugebauer R, Schlicksupp A, Kirsch J, Kuhse J. Activity-dependent shedding of the NMDA receptor glycine binding site by matrix metalloproteinase 3: a PUTATIVE mechanism of postsynaptic plasticity. PLoS One. 2008; 3:e2681. [PubMed: 18629001]

Szklarczyk A, Ewaleifoh O, Beique JC, Wang Y, Knorr D, Haughey N, Malpica T, Mattson MP, Huganir R, Conant K. MMP-7 cleaves the NR1 NMDA receptor subunit and modifies NMDA receptor function. Faseb J. 2008; 22:3757–3767. [PubMed: 18644839]

Larsen PH, DaSilva AG, Conant K, Yong VW. Myelin formation during development of the CNS is delayed in matrix metalloproteinase-9 and -12 null mice. J Neurosci. 2006; 26:2207–2214. [PubMed: 16495447]

Griffiths IR, McCulloch MC. Nerve fibres in spinal cord impact injuries. Part 1. Changes in the myelin sheath during the initial 5 weeks. J Neurol Sci. 1983; 58:335–349. [PubMed: 6842262]

Nakamura M, Zhou XZ, Lu KP. Critical role for the EB1 and APC interaction in the regulation of microtubule polymerization. Curr Biol. 2001; 11:1062–1067. [PubMed: 11470413]

Lytle JM, Wrathall JR. Glial cell loss, proliferation and replacement in the contused murine spinal cord. Eur J Neurosci. 2007; 25:1711–1724. [PubMed: 17432960]

Alonso G. NG2 proteoglycan-expressing cells of the adult rat brain: possible involvement in the formation of glial scar astrocytes following stab wound. Glia. 2005; 49:318–338. [PubMed: 15494983]

Zawadzka M, Rivers LE, Fancy SP, Zhao C, Tripathi R, Jamen F, Young K, Goncharevich A, Pohl H, Rizzi M, Rowitch DH, Kessaris N, Suter U, Richardson WD, Franklin RJ. CNS-resident glial progenitor/stem cells produce Schwann cells as well as oligodendrocytes during repair of CNS demyelination. Cell Stem Cell. 2010; 6:578–590. [PubMed: 20569695]

Toma JS, McPhail LT, Ramer MS. Differential RIP antigen (CNPase) expression in peripheral ensheathing glia. Brain Res. 2007; 1137:1–10. [PubMed: 17229407]

Buss A, Pech K, Kakulas BA, Martin D, Schoenen J, Noth J, Brook GA. Matrix metalloproteinases and their inhibitors in human traumatic spinal cord injury. BMC Neurol. 2007; 7:17. [PubMed: 17594482]

de Castro RC Jr. Burns CL, McAdoo DJ, Romanic AM. Metalloproteinase increases in the injured rat spinal cord. Neuroreport. 2000; 11:3551–3554. [PubMed: 11095516]

Moore CS, Milner R, Nishiyama A, Frausto RF, Serwanski DR, Pagarigan RR, Whitton JL, Miller RH, Crocker SJ. Astrocytic Tissue Inhibitor of Metalloproteinase-1 (TIMP-1) Promotes Oligodendrocyte Differentiation and Enhances CNS Myelination. J Neurosci. 2011; 31:6247–6254. [PubMed: 21508247]

Oh LY, Larsen PH, Krekoski CA, Edwards DR, Donovan F, Werb Z, Yong VW. Matrix metalloproteinase-9/gelatinase B is required for process outgrowth by oligodendrocytes. J Neurosci. 1999; 19:8464–8475. [PubMed: 10493747]

Uhm JH, Dooley NP, Oh LY, Yong VW. Oligodendrocytes utilize a matrix metalloproteinase, MMP-9, to extend processes along an astrocyte extracellular matrix. Glia. 1998; 22:53–63. [PubMed: 9436787]

Manabe S, Gu Z, Lipton SA. Activation of matrix metalloproteinase-9 via neuronal nitric oxide synthase contributes to NMDA-induced retinal ganglion cell death. Invest Ophthalmol Vis Sci. 2005; 46:4747–4753. [PubMed: 16303975]

Chattopadhyay S, Shubayev VI. MMP-9 controls Schwann cell proliferation and phenotypic remodeling via IGF-1 and ErbB receptor-mediated activation of MEK/ERK pathway. Glia. 2009; 57:1316–1325. [PubMed: 19229995]

Gijbels K, Proost P, Masure S, Carton H, Billiau A, Opdenakker G. Gelatinase B is present in the cerebrospinal fluid during experimental autoimmune encephalomyelitis and cleaves myelin basic protein. J Neurosci Res. 1993; 36:432–440. [PubMed: 7505841]

Proost P, Van Damme J, Opdenakker G. Leukocyte gelatinase B cleavage releases encephalitogens from human myelin basic protein. Biochem Biophys Res Commun. 1993; 192:1175–1181. [PubMed: 7685161]

Busch SA, Hamilton JA, Horn KP, Cuascut FX, Cutrone R, Lehman N, Deans RJ, Ting AE, Mays RW, Silver J. Multipotent adult progenitor cells prevent macrophage-mediated axonal dieback and promote regrowth after spinal cord injury. J Neurosci. 2011; 31:944–953. [PubMed: 21248119]

Rosenberg MM, Yang F, Giovanni M, Mohn JL, Temburni MK, Jacob MH. Adenomatous polyposis coli plays a key role, in vivo, in coordinating assembly of the neuronal nicotinic postsynaptic complex. Mol Cell Neurosci. 2008; 38:138–152. [PubMed: 18407517]

Lehmann HC, Kohne A, Bernal F, Jangouk P, Meyer Zu Horste G, Dehmel T, Hartung HP, Previtali SC, Kieseier BC. Matrix metalloproteinase-2 is involved in myelination of dorsal root ganglia neurons. Glia. 2009; 57:479–489. [PubMed: 18814268]

- This study offers the first evidence that MMP-9 controls NG2+ cell division in CNS.
- MMPs control the NG2 proteoglycan and NMDA receptor shedding in spinal cord.
- Acute MMP-9 block allows for oligodendrocyte maturation and remyelination of spinal cord.
- Acute MMP-9 inhibition improves functional recovery after spinal cord injury.

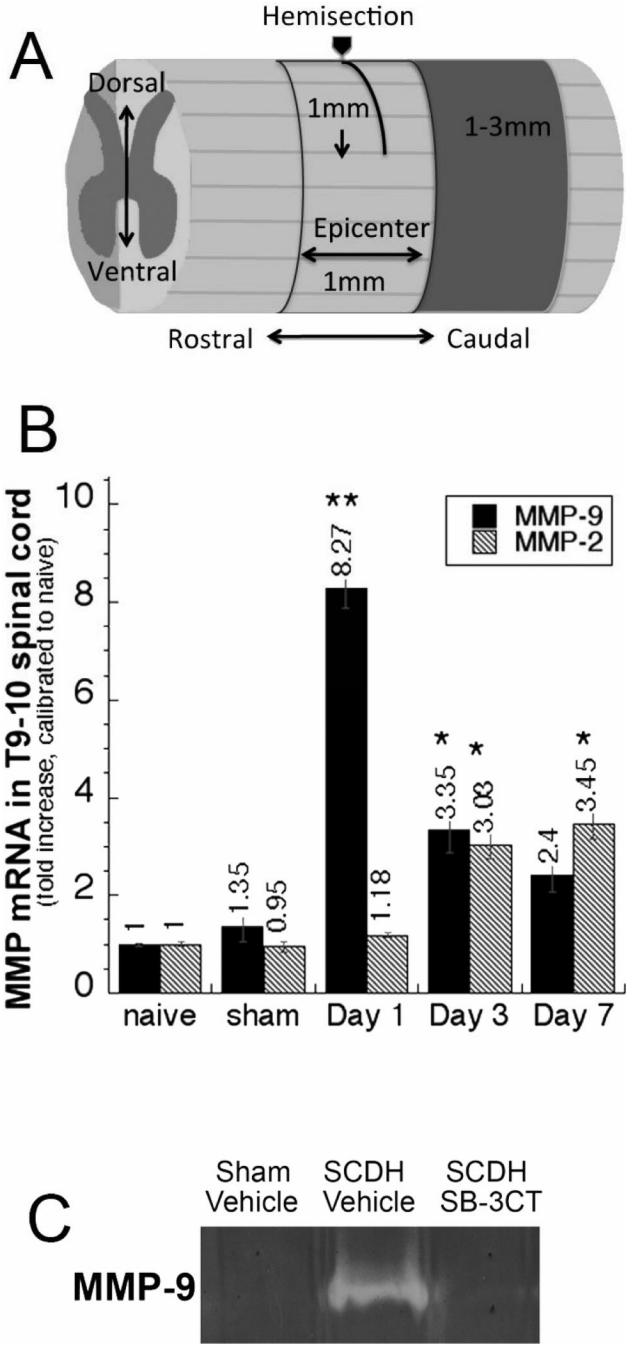

Figure 1. MMP-2 and MMP-9 expression after spinal cord injury

A, A schematic illustration of T9-10 SCDH lesion. **B**, *Taqman* qRT-PCR for MMP-2 and MMP-9 in T9-10 spinal cords after SCDH or sham surgery. Values displayed are the mean relative mRNA of N=4/group, normalized to GAPDH and calibrated to naïve cord ± SEM (*, $p<0.05$; **, $p<0.01$, ANOVA and Tukey's post-hoc test). **C**, Gelatin zymography for MMP-9 in the epicenter and peak (1 day) of SCDH or sham surgery after vehicle or SB-3CT (10 mk/kg/day, i.p.) administered immediately after the surgery.

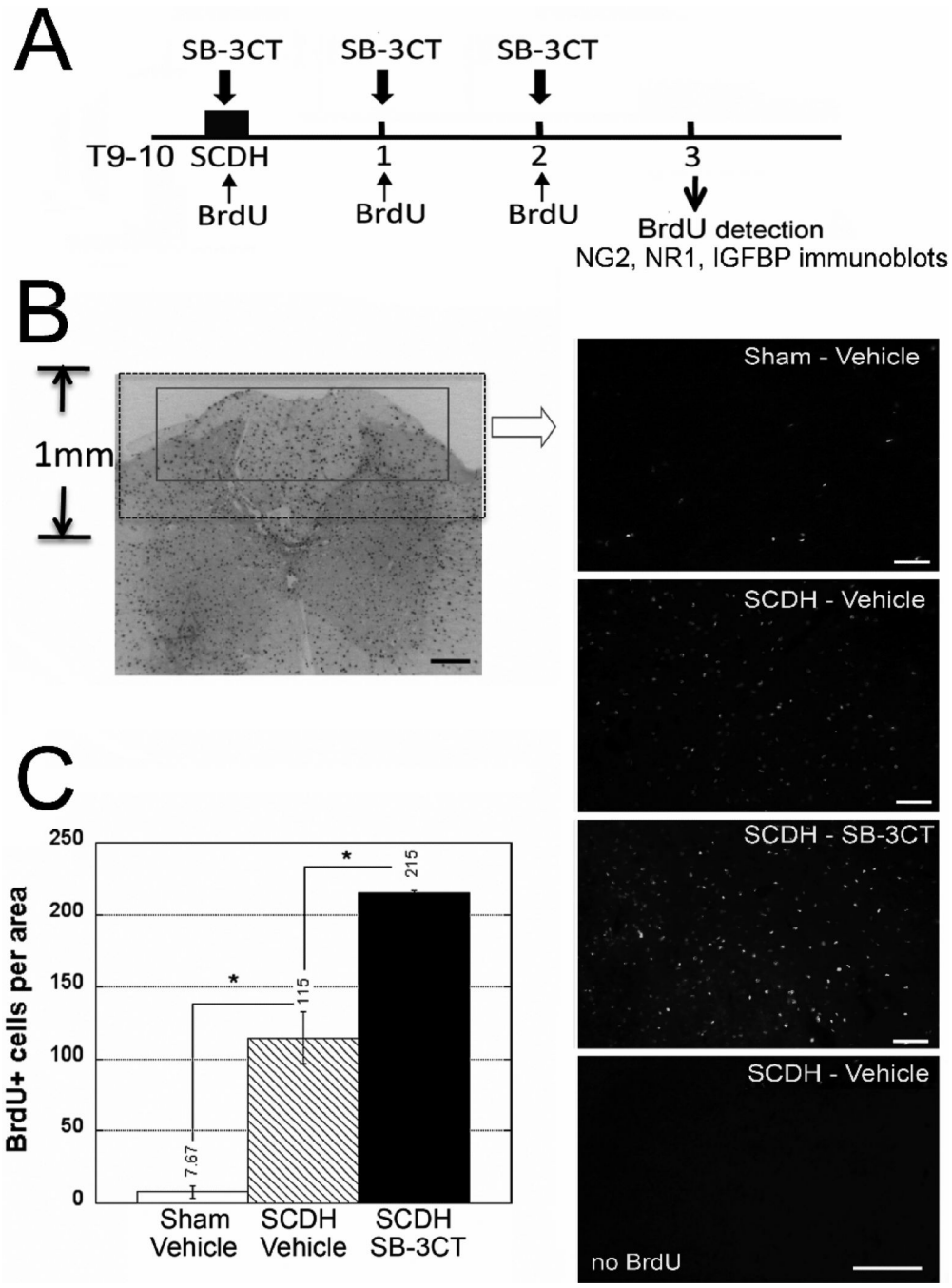

Figure 2. Acute MMP-9 inhibition promotes cell division

A, Experimental schedule for intraperitoneal SB-3CT (10 mg/kg/day) or vehicle (10% DMSO), and BrdU (50 mg/kg/day) or its vehicle (saline) administration immediately, and then daily for 2 days after SCDH, followed by BrdU detection and immunoblotting at 3 days after the surgery and/or therapy. **B**, BrdU immunofluorescence in the spinal cord. The box outlines the area used to quantify BrdU+ profiles (inverted image at objective magnification 5x, scale bar = 20 μm). Representative micrographs of sham-operated or SCDH spinal cords after SB-3CT or vehicle treatment and SCDH spinal cords of vehicle without BrdU injection. Scale bar = 55 μm. **C**, The number of BrdU+ cells is elevated 14-fold after SCDH relative to sham. In the injured spinal cord, acute SB-3CT therapy increases the rate of cell

mitosis 1.8-fold compared with vehicle. Values displayed are mean ± SEM per area (55 $\times 10^3$ μm^2) of N=4/group, 5-7 sections per N spaced 125 μm apart from a dorsal spinal cord 1-3 mm caudal to the epicenter (*, $p<0.05$, AVOVA and Tukey's post-hoc test).

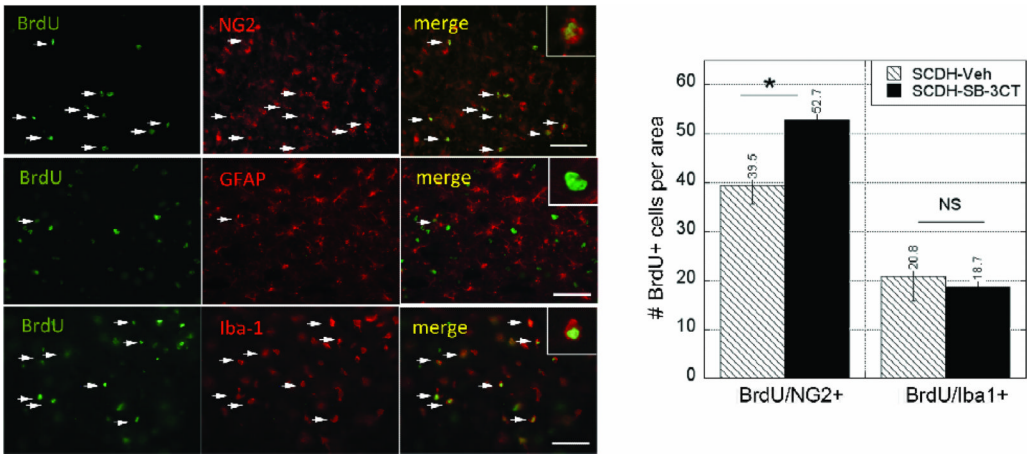

Figure 3. MMP-9 controls NG2 cell mitosis

BrdU+ cells (green) dual-labeled with NG2, GFAP or Iba-1 (red) at 3 days after SCDH and SB-3CT therapy demonstrating representative co-localization signals (arrows). Note that BrdU+ cells are mainly, NG2+ progenitors and Iba-1+ microglia/astrocytes, as GFAP+ astocytes contribute minimally. Scale bar = 55 μm. The graph represents the mean ± SEM per area (55×10^3 μm^2) of N=4-7/group, 5-10 sections per N, spaced 125 μm apart from a dorsal cord 1-3 mm caudal to the epicenter (*, $p<0.05$, AVOVA and Tukey's post-hoc test). Acute SB-3CT therapy selectively increases the number of dividing NG2 but not Iba-1-reactive cells. The regiment for BrdU, SB-3CT or vehicle treatments is specified in Fig 2A.

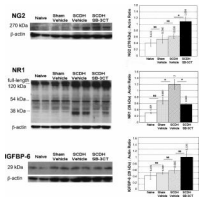

Figure 4. MMPs controls NR1 and NG2 levels in spinal cord

Immunoblotting for NG2, NR1 and IGFBP-6 at 3 days after SCDH and acute SB-3CT (10mg/kg) or vehicle (10% DMSO) treatment. The graphs represents the mean OD of the specified band to β-actin ratio ± SEM in N=4 rats/group (*, $p<0.05$, ANOVA).

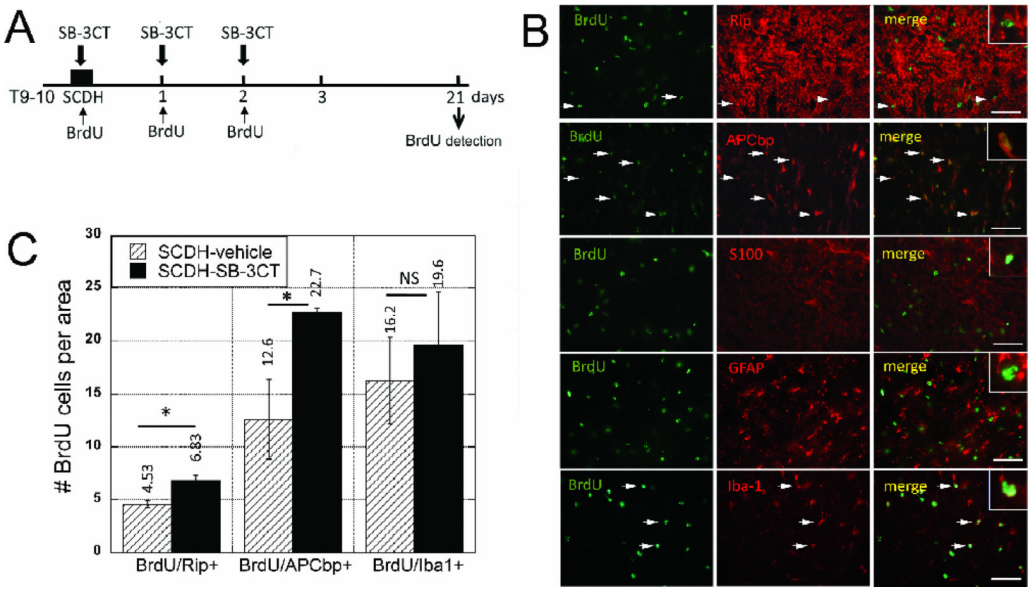

Figure 5. Post-mitotic cell profiles in remyelinating spinal cords

A, Experimental schedule for SB-3CT (10 mg/kg/day, i.p.) and BrdU (50 mg/kg/day i.p.) administration immediately, and then daily for 2 days after SCDH, followed by BrdU detection at 21 days after the surgery and/or therapy. **B**, BrdU+ cells, dual-labeled with Rip, APC end-binding protein 1 (APCbp), or Iba-1 at 21 days after SCDH. Values displayed are mean ± SEM per area (55 $\times 10^3$ μm^2) of N=5/group, 5-10 sections per N, spaced 125 μm apart from a dorsal spinal cord 1-3 mm caudal to the epicenter (*, $p<0.05$, AVOVA and Tukey's post-hoc test). The number of post-mitotic OLs but not microglia/macrophages is increased after SB-3CT therapy. **C**, Representative micrographs of BrdU+ cells (green) with Rip, APCbp, GFAP, S100 and Iba-1 (red) used for quantification in B. Co-localization, observed in Rip and APCbp, but not GFAP or S100 reactive cells. Scale bar = 55 μm.

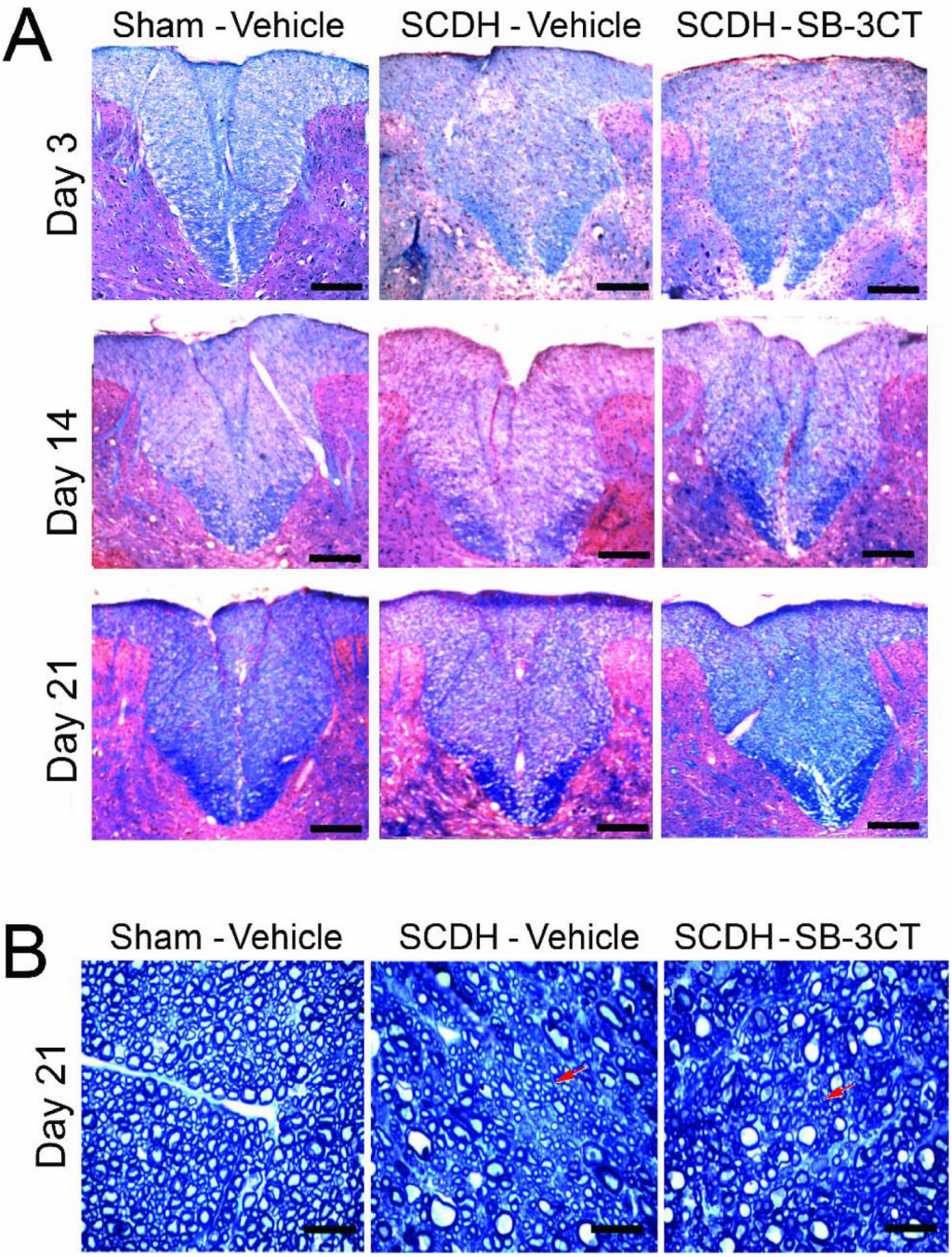

Figure 6. Myelin neuropathology after acute MMP-9/2 block

A, Luxol fast blue and H&E staining for myelin (blue) after SCDH. A gradual, time-dependent myelin loss is observed in the dorsal column of the injured, vehicle-treated spinal cords. After acute SB-3CT therapy myelin content increased at 3, 14 and 21 days after SCDH compared to the vehicle-treated cords. Representative micrographs of N=4/group, 5-10 sections per N, spaced 125 μm apart from a dorsal spinal cord 1-3 mm caudal to the epicenter. Scale bars = 10 μm. **B**, Methylene Blue Azure II stained araldite sections 21 days after SCDH. Characteristically circular axonal profiles, surrounded by a compact rim of myelin sheaths are observed in sham-operated cords. Clusters of well-packed areas of small-diameter axons, surrounded by the thin rim of myelin sheaths indicate, presumably,

remyelinating areas (arrows). Representative micrographs of 8 sections/group from a spinal cord 1-3 mm caudal to the epicenter at objective magnification 100x (scale bars = 20 μm).

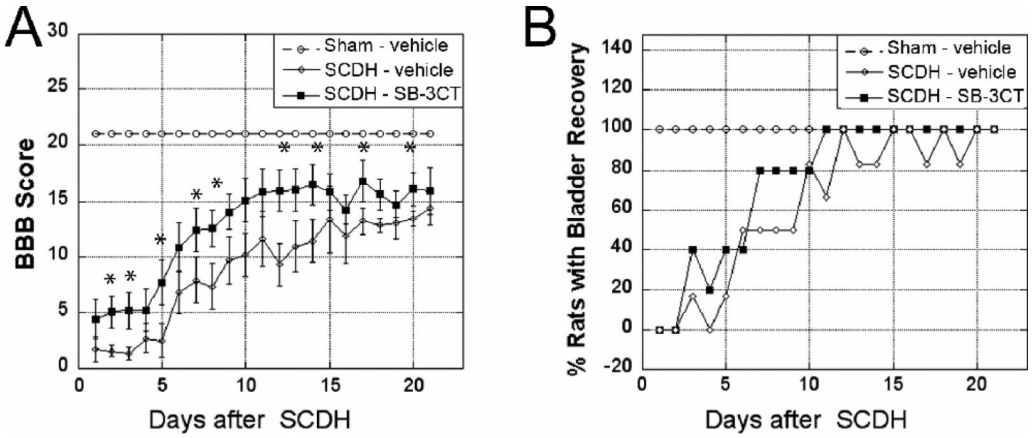

Figure 7. Functional recovery improves with acute MMP-9/2 blockade

A, Locomotor recovery using BBB scale after acute SB-3CT (10 mg/kg/day) or vehicle (10% DMSO) treatment administered i.p. immediately after SCDH or sham operation, and then daily for two days. Values displayed are mean scores ± SEM of N=8-11/group, *, $p<0.05$ at each analyzed time-point (ANOVA, Tukey's post-hoc test). **B**, Bladder recovery assessment after SCDH or sham surgery. A rapid and stable improvement of somatosensory recovery is noted after acute SB-3CT therapy relative to vehicle treatment. Values displayed are mean % of animals with bladder recovery of N=6/group.